



## Heterogeneous reaction kinetics influencing benzo(a)pyrene global atmospheric distribution and related lifetime lung cancer risk

Mega Octaviani<sup>1,2,§,\*</sup>, Benjamin A. Musa Bandowe<sup>1</sup>, Qing Mu<sup>1,3</sup>, Jake Wilson<sup>1</sup>, Holger  
5 Tost<sup>4</sup>, Hang Su<sup>5</sup>, Yafang Cheng<sup>1</sup>, Manabu Shiraiwa<sup>6</sup>, Ulrich Pöschl<sup>1</sup>, Thomas  
Berkemeier<sup>1,\*</sup>, Gerhard Lammel<sup>1,7,\*</sup>

<sup>1</sup>Max Planck Institute for Chemistry, Multiphase Chemistry Department, Mainz, Germany

<sup>2</sup>Karlsruhe Institute of Technology, Institute of Meteorology and Climate Research,  
10 Department Troposphere Research, Karlsruhe, Germany

<sup>3</sup>Xi'an Jiaotong-Liverpool University, Department of Health and Environmental Sciences,  
Suzhou, China

<sup>4</sup>University of Mainz, Institute of Atmospheric Physics, Mainz, Germany

<sup>5</sup>Key Laboratory of Atmospheric Environment and Extreme Meteorology, Institute for  
15 Atmospheric Physics, Chinese Academy of Science, Beijing, China

<sup>6</sup>University of California, Irvine, Department of Chemistry, Irvine, CA, USA

<sup>7</sup>Masaryk University, Research Centre for Toxic Compounds in the Environment, Brno, Czech  
Republic

20 <sup>§</sup>Now at: Swedish Meteorological and Hydrological Institute, Norrköping, Sweden

\*Correspondence to mega.octaviani@smhi.se, t.berkemeier@mpic.de, g.lammel@mpic.de

### Abstract

25 Benzo(a)pyrene (BaP) is a ubiquitous and hazardous air pollutant that increases the risk of lung cancer. Heterogeneous oxidation by ozone limits the atmospheric concentrations and long-range transport potential of BaP, but the actual oxidation rates and chemical lifetimes of BaP under varying atmospheric conditions are not yet well constrained. In this study, we employ the ECHAM/MESSEy atmospheric chemistry model for the simulation of semivolatile organic  
30 compounds (using the SVOC submodel) with coupled surface compartments to compare four different kinetic schemes of BaP oxidation and assess the pollutant's global distribution and associated lung cancer risks. We find that a kinetic scheme considering the temperature and humidity dependence of particle phase state, mass transport, and reaction rate coefficient is



35 best suited to reproduce ambient observations, yielding mean global atmospheric lifetime and  
total environmental residence times of ~5 hours and ~20 days, respectively. Estimates of the  
BaP-related lung cancer risk surpass  $10^{-5}$  (i.e., 10 excess cases per million people) in central  
and eastern Europe, parts of the Russian Far East, northern India, Pakistan, and western China,  
and surpass  $10^{-4}$  in central, eastern, and northeastern China.

#### 40 **1. Introduction**

The polycyclic aromatic hydrocarbon benzo(a)pyrene (BaP) is one of the most prominent  
organic air pollutants and hazardous constituents of fine particulate matter.<sup>1-3</sup> BaP is classified  
as a human carcinogen by the International Agency for Research on Cancer.<sup>4</sup> The concentration  
of BaP in particulate matter is regulated in the air quality guidelines of the European Union and  
45 other countries.<sup>5, 6</sup> The atmospheric distribution of BaP has been investigated in numerous  
studies, but the degradation rate in the atmosphere remains a major uncertainty in determining  
the atmospheric burden and human exposure to BaP.<sup>7-13</sup> Due to its low volatility, BaP resides  
primarily in the particulate phase of atmospheric aerosols, and the heterogeneous oxidation by  
ozone is more effective than gas-phase chemistry for its chemical transformation. The  
50 degradation rate of BaP depends strongly on both the heterogeneous reaction rate coefficient,  
which varies across chemical composition of coexisting aerosols, and the accessibility of BaP  
molecules to oxidants, which is influenced by particle phase state.<sup>9, 12, 14-16</sup> Inhalation exposure  
to polycyclic aromatic hydrocarbons is known to increase the risk of lung cancer and, recently,  
global chemistry-transport models have been used to derive lung cancer risk from global  
55 atmospheric distribution.<sup>16-19</sup> Although it has been determined that the health burden of PAHs  
is prominently concentrated in urban areas, investigation into the sensitivity and uncertainty  
related to the choice of different heterogeneous reaction schemes is lacking in existing studies.  
Furthermore, the reaction of BaP with  $O_3$  can result in the formation of highly toxic oxygenated  
products such as quinones, epoxides, and hydroxylated BaPs.<sup>20-23</sup> The accumulation of  
60 oxygenated BaPs in aerosols results in enhanced bioavailability/bioaccessibility and toxicity.<sup>21,</sup>  
24-26

Thus, a quantitative understanding of the heterogeneous reaction between BaP and  $O_3$  in the  
global atmosphere is a major step towards the assessment of the human health risk posed by  
65 BaP and its transformation products. In this study, we employ a global atmospheric chemistry  
model to investigate how different heterogeneous oxidation schemes influence the global



atmospheric distribution and environmental fate of BaP and how these reflect on lung cancer risk.

## 70 2. Methods

The global climate and chemistry model EMAC (ECHAM5/MESSy Atmospheric Chemistry)<sup>27, 28</sup> was applied with the SVOC submodel for the simulation of semivolatile organic compounds.<sup>12, 29</sup>

75 EMAC is a numerical chemistry and climate simulation system that includes sub-models describing tropospheric and middle atmosphere processes and their interaction with oceans, land and human influences.<sup>27</sup> It uses the second version of the Modular Earth Submodel System (MESSy2) to link multi-institutional computer codes. The core atmospheric model is the 5th generation European Centre Hamburg general circulation model (ECHAM5).<sup>30</sup> The physics  
80 subroutines of the original ECHAM code have been modularized and reimplemented as MESSy submodels and have continuously been further developed. Only the spectral transform core, the flux-form semi-Lagrangian large scale advection scheme, and the nudging routines for Newtonian relaxation are remaining from ECHAM. For the present study we applied EMAC (MESSy version 2.50.0) in the T42L19 resolution, i.e. with a spherical truncation of  
85 T42 (corresponding to a quadratic Gaussian grid of approx. 2.8°×2.8° in latitude and longitude) with 19 vertical hybrid pressure levels up to 10 hPa. The applied model setup comprised various submodels including for online ozone chemistry through the MECCA<sup>31</sup> gas-phase chemical kinetics, aerosol microphysics and composition (GMXE)<sup>32</sup>, as well as representations for semi-volatile organic compounds. Note that the applied SVOC submodel (and the corresponding  
90 model configuration as described in Octaviani et al.<sup>29</sup>) adopts a species-based approach to explicitly simulate the partitioning and fate of organic aerosols in multiple environmental compartments. SVOC is not to be mixed up with the ORACLE submodel<sup>33</sup>, which takes a comprehensive bulk-based approach, using volatility and oxygen-to-carbon basis sets to simulate the partitioning and chemical aging of organic aerosols in the atmosphere.

95

The simulations covered the period 2007-2009, which was preceded by a one-year spin-up period. The emissions of BaP were taken from the global inventory of Shen et al.<sup>34</sup> for the base year 2008 with a total of 4509 Mg per year. We incorporated monthly factors for seasonality, derived from the black carbon anthropogenic emissions in the IPCC's Representative



100 Concentration Pathway (RCP) 6.0 emission scenario.<sup>35</sup> Additionally, an entry split of 5%  
release to the gas phase and 95% to the particulate phase was employed, with re-partitioning  
occurring for every time step. This choice aligns with BaP's low volatility and is consistent  
with the approach used in the previous studies.<sup>12, 29</sup>

105 In the SVOC submodel, the particulate phase of BaP was described using seven lognormal  
modes, four hydrophilic and three hydrophobic modes.<sup>29</sup> The hydrophilic modes cover the full  
particle size spectrum (i.e., nucleation, Aitken, accumulation, and coarse mode), while a  
hydrophobic nucleation mode was omitted. Aerosol microphysical processes and interactions  
with background aerosol are determined with the help of the GMXe aerosol submodel of  
110 EMAC.<sup>32</sup> BaP transported with individual modes are treated explicitly as separate tracers. In  
the simulations, particulate phase BaP was emitted to the hydrophobic Aitken mode. The  
SVOC submodel calculates the partitioning of organic compounds between the gas and  
particulate phases using poly-parameter linear free energy relationships (ppLFER),<sup>36, 37</sup> where  
the partition coefficient is defined as the sum of individual partition coefficients representing  
115 surface adsorption and bulk-phase absorption processes to inorganic and organic aerosols.  
Besides removal through dry and wet deposition, BaP is subject to heterogeneous oxidation by  
ozone. Gas-phase oxidation is switched off as BaP predominantly resides in the particulate  
phase, accounting for at least 90% of the total mass.

120 In this study, we tested and compared four different kinetic schemes of heterogeneous oxidation  
by ozone. Firstly, the recently developed Reactive Oxygen Intermediate-Temperature  
dependent (ROI-T) scheme of Mu et al. 2018<sup>12</sup>, which accounts for the formation of ROI upon  
decomposition of adsorbed ozone<sup>38</sup> and the influence of temperature and relative humidity on  
the first-order reaction rate coefficient. In ROI-T, BaP is rapidly oxidized under warm and  
125 humid conditions due to rapid diffusion in liquid particles, but effectively shielded from  
degradation under cold and dry conditions caused by slow diffusion in semi-solid or solid  
particles. The scheme builds on the results of several experimental and theoretical studies.<sup>15, 38-  
44</sup> The required kinetic parameters are summarized in the Supporting Information Table S1.  
The other three kinetic schemes are based on laboratory studies of BaP degradation on different  
130 substrates without functional dependence on temperature and humidity: the Pöschl et al. 2001<sup>45</sup>  
scheme represents an upper limit of reactivity based on the surface reaction of ozone with BaP  
on soot aerosol particles; the Kwamena et al. 2004<sup>46</sup> scheme represents an intermediate level  
of reactivity based on the reaction of ozone with BaP on organic aerosol particles; and the



135 Kahan et al. 2006<sup>47</sup> scheme represents a lower limit of reactivity based on the reaction of ozone  
with BaP in organic films. The different degradation rates of these laboratory-derived schemes  
are summarized in Table S2. For the chemical degradation of BaP on ground surfaces (soil and  
vegetation) and in the ocean surface layer, first-order rate coefficients of  $2.55 \times 10^{-8} \text{ s}^{-1}$  and  
 $1.30 \times 10^{-9} \text{ s}^{-1}$  were assumed, respectively.<sup>48, 49</sup>

### 140 3. Results and Discussion

#### *Global distribution*

Figures 1 and S1 show the average near-surface concentration and total atmospheric column  
of BaP, calculated using four different kinetic schemes. With the Mu et al. 2018 (ROI-T)  
scheme (Figures 1a and S1a), high atmospheric concentrations and column burdens of BaP  
145 ( $>10 \text{ pg m}^{-3}$  or  $>0.1 \text{ kg per } 2.8 \times 2.8^\circ$  grid cell, respectively) are predominantly obtained in  
densely populated and industrialized regions with strong emissions from fossil fuel combustion  
– such as China, India, Europe, and the eastern US – and in regions with strong biomass burning  
emissions from vegetation and peat fires, especially in the tropics (Brazil, central Africa,  
Indonesia). The substantial BaP burden over the Arctic, North Atlantic, and northern Pacific  
150 Ocean ( $\sim 1 \text{ pg m}^{-3}$  or  $\sim 0.01 \text{ kg per grid cell}$ ) is caused by long-range transport from North  
America, Europe, and Asia, and is enabled by shielding effects of highly viscous organic  
coatings under low temperatures and relative humidity.<sup>50, 51</sup> In contrast, very low near-surface  
concentrations and atmospheric burden are obtained over the tropical southern Oceans due to  
short lifetimes and large distances to emission sources. As expected, the lowest burden is seen  
155 over Antarctica at large distances from the fossil fuel and biomass burning sources ( $<10^{-3} \text{ pg}$   
 $\text{m}^{-3}$  or  $<10^{-4} \text{ kg per grid cell}$ ). This is in agreement with observation-based studies reporting  
that substantial amounts of BaP are reaching the Arctic<sup>52, 53</sup> but not the Antarctic.<sup>54, 55</sup>

With the Kwamena et al. 2004 scheme (Figures 1b and S1b), we obtain a similar atmospheric  
160 concentration and burden of BaP as with the ROI-T scheme, but the spatial distribution patterns  
are regionally different. This is because the temperature-dependence and humidity-dependence  
(i.e., shielding effects of organic coatings) are only represented in the ROI-T scheme, but not  
in the Kwamena et al. 2004 scheme. Consequently, the atmospheric burden in the polar regions  
is higher with the ROI-T scheme, owing to the low average temperature and humidity leading  
165 to a slow BaP degradation rate in a highly viscous particle phase state. On the other hand, the  
Kahan et al. 2006 scheme represents a lower limit of BaP reactivity and with a long atmospheric



lifetime due to chemistry of about one week (Table S4). Here, concentrations and burdens are (on average) two orders of magnitude higher than with the ROI-T scheme (Figures 1c and S1c). Accordingly, this scheme enables significant long-range transport of BaP. For example, we see  
170 a more pronounced influence of continental sources on marine BaP concentrations, in contrast to other schemes where emissions from shipping lead to clearly defined ship tracks. Furthermore, the Pöschl et al. 2001 scheme, which represents an upper limit of reactivity, yields much lower concentrations (approximately by one order of magnitude on average), with a spatial pattern closely resembling the pattern of BaP emissions (Figure 1d). When ozone  
175 concentrations are higher than 150  $\mu\text{g}/\text{m}^3$ , after one hour, the BaP concentration can be reduced up to 80% in the Kahan et al. 2006 scheme and 20% in the Pöschl et al. 2001 scheme. This reflects a particularly short atmospheric lifetime of only minutes for BaP due to chemistry (Table S4).

180

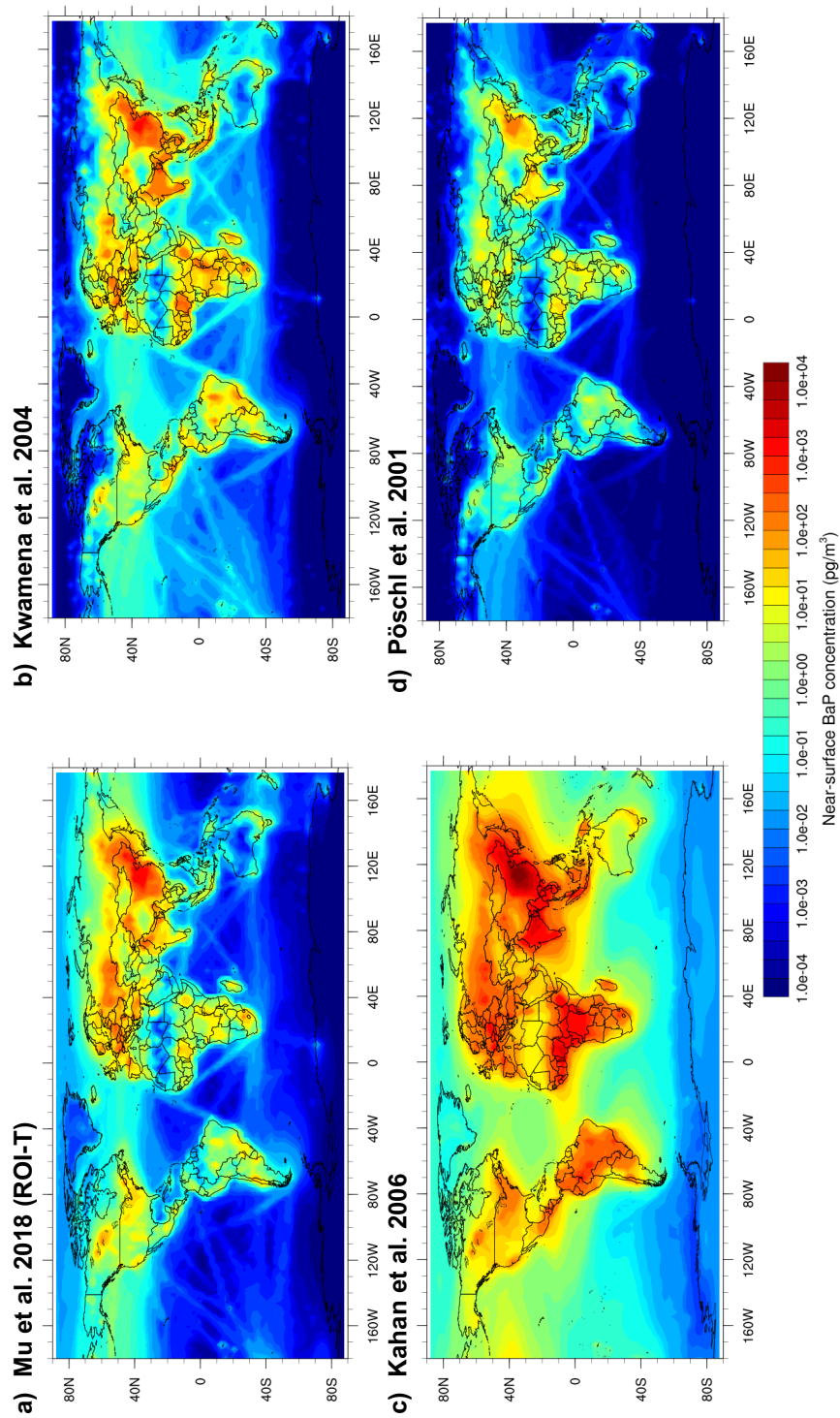


**Figure 1.** Global near-surface atmospheric concentrations of BaP ( $\text{pg m}^{-3}$ ) averaged over 2007-2009 using different kinetic schemes of heterogeneous oxidation: (a) Mu et al. 2018 (ROI-T), (b) Kwamena et al. 2004, (c) Kahan et al. 2006, (d) Pöschl et al. 2001.



The comparison of field measurement data with the ROI-T scheme demonstrates improved agreement between global model results and observations in both source and remote regions (Figures S2-S3), also discussed in Mu et al.<sup>12</sup>. The model results obtained with the ROI-T scheme come much closer to observations at Arctic stations compared to the Kwamena et al. 2004 and Pöschl et al. 2001 schemes (Figures S2-S3), enabling better treatment of the long-range transport. Although the Kahan et al. 2006 scheme comes closest to the mean and median observations at the Arctic stations, it generally overestimates BaP concentrations in other locations and during Arctic summer months. A conservative overall estimate of uncertainty follows from the lower and upper limit values obtained with the Pöschl et al. 2001 and Kahan et al. 2006 schemes. As a more realistic estimate of uncertainty, however, we suggest using the difference between the ROI-T scheme (which is physicochemically more realistic and in better agreement with global observations<sup>12</sup>) and the Kwamena et al. 2004 scheme (an alternative estimate of intermediate reactivity and has been used in many regional/global modeling studies<sup>8, 29, 56-59</sup>).

### ***Vertical profiles***

Figure 2A shows vertical profiles of BaP mass mixing ratio averaged globally. All schemes except the Kahan et al. 2006 scheme demonstrate a steep decrease in BaP concentrations with increasing altitude across the planetary boundary layer (up to ~3 km/~700 hPa). In the free troposphere (up to ~15 km, ~100 hPa), temperature and humidity are generally lower. As a result, the ROI-T scheme yields a more gradual decrease in concentration, while the temperature and humidity-independent Kwamena et al. 2004 and Pöschl et al. 2001 schemes show a stronger decrease. On the other hand, the low reactivity of the Kahan et al. 2006 scheme results in an overall much smaller BaP decrease with altitude. Differences between the schemes for different parts of the world are discussed in the Supporting Information S4.

### ***Burden and lifetime***

The global and regional total atmospheric column burden of BaP are presented in Table S3 as absolute and relative values. The global BaP burden obtained with the ROI-T scheme is ~1.6 Mg (Table S3a), of which 84% is concentrated in the northern mid-latitudes (Table S3b) and 42% in the planetary boundary layer below ~1.5 km altitude (850 hPa). With the other kinetic schemes, the global atmospheric burdens of BaP range from a 16 times lower limit of ~0.1 Mg (Pöschl et al. 2001) via a 50% lower value of ~0.8 Mg (Kwamena et al. 2004) to a 40





times higher upper limit of ~64 Mg (Kahan et al. 2006). Most of the BaP burden predicted by these schemes is found to reside in the tropics (47-66%). The much lower fraction of the BaP burden predicted for the tropics under the ROI-T scheme (~14%) is due to faster degradation at high temperature and humidity.

The atmospheric (photo-)chemical lifetime of BaP, in the following just referred to as atmospheric lifetime, is calculated as the ratio of atmospheric burden (in  $\text{pg m}^{-2}$ ) to its chemical loss rate (in  $\text{pg m}^{-2} \text{h}^{-1}$ ). These lifetimes are calculated on both the global and regional scale as well as annual and seasonal means (Table S4). Lammel et al.<sup>7</sup> previously estimated a global atmospheric lifetime for BaP of ~48 h without considering heterogeneous degradation and ~0.17 h when accounting for it. On the other hand, Shrivastava et al.<sup>16</sup> considered coating of BaP containing aerosols with organics, providing viscosity-dependent shielding from ozone oxidation and resulting in an atmospheric lifetime estimate of ~5 days (120 h), as opposed to ~2 h without shielding. These estimates significantly differ from our estimated global atmospheric lifetime (mean value from 2007-2009) using the ROI-T scheme of about 5 h. The difference to Lammel et al.<sup>7</sup> can be attributed to differences in the scheme for heterogeneous chemistry. Their study employed reaction rate coefficients independent of temperature and humidity for particulate BaP oxidation, only allowed for reaction with OH and NO<sub>3</sub>, and used a different method for gas-particle partitioning i.e., considering interaction with black carbon and organic matter. Our study implemented the ppLFFER method, which not only considers interactions with black carbon and organic matter, but also considers interactions with various other particulate matter constituents. The differences with Shrivastava et al.<sup>16</sup> arise because the BaP heterogeneous kinetics are fully turned off at  $T \leq 296 \text{ K}$  or relative humidity  $\leq 50\%$  in their study, whereas in the ROI-T scheme they are gradually slowed down as a function of temperature and humidity. The differences in atmospheric burdens and lifetime as well as their spatial distribution patterns highlight the importance of temperature- and humidity-dependent treatment of aerosol phase and heterogeneous reaction rate coefficients in determining global atmospheric transport and distribution of hazardous pollutants.<sup>3, 12, 16, 42</sup>

Across latitudinal zones, atmospheric lifetime varies by more than an order of magnitude i.e., 1.8 h in the Tropics and 43.5 h in the Antarctic (ROI-T; Table S4). The Kahan et al. 2006 and Pöschl et al. 2001 schemes yield the longest and shortest lifetimes, respectively, i.e., 155.5 and 0.08 h as the global annual means, 164.2 and 0.1 h in the Arctic, and 224.2 and 0.12 h in the

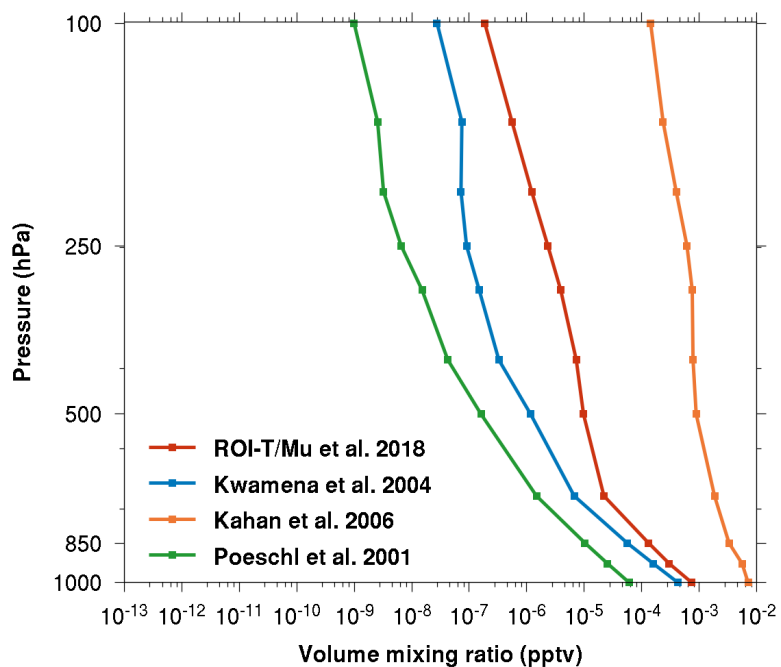


Antarctic. This 50% increase from the global mean to the Antarctic lifetime under the Pöschl et al. 2001 scheme is caused solely by the reduced regional O<sub>3</sub> concentration, as the scheme neglects the effects of temperature and humidity. The ROI-T scheme demonstrates that the atmospheric lifetime is significantly enhanced due to the lower temperature and humidity in the Antarctic (43.5 h) compared to the Arctic (~12 h). For other climatic regions, the calculated lifetime increases from the tropics to higher latitudes (Table S4). These lifetime trends imply that BaP will accumulate more in the polar regions and thus endanger vulnerable marine ecosystems. The seasonal signal, i.e., the atmospheric lifetime in winter over lifetime in summer, ranges from 10-13 in northern high- and mid-latitude regions and is ~2 in the tropics and southern hemisphere.

More than 99% of BaP mass is stored in soils, oceans, vegetation, snow, and glaciers (Table S5). Therefore, in the following, we will investigate the total burden in these surface compartments. We find that the total surface burden and distribution are highly dependent on the atmospheric degradation scheme (see Supporting Information S5 for more details). This implies that the selected atmospheric degradation scheme has a major impact on BaP's environmental fate, overall environmental persistence, long-range transport potential, and consequently human and ecosystem exposure in remote environments. Thus, it is important to use an accurate representation of the reactivity of BaP in air for environmental and human health risk assessment. Compared to the global atmospheric burden of ~1.6 Mg BaP (Table S3), the total burden in surface compartments is ~249 Mg under the ROI-T scheme (Table S5). This total environmental burden (atmosphere and surface) is fed by ~4500 Mg per year of global emissions, hence, corresponds to an environmental residence time of the pollutant of ~20 days.

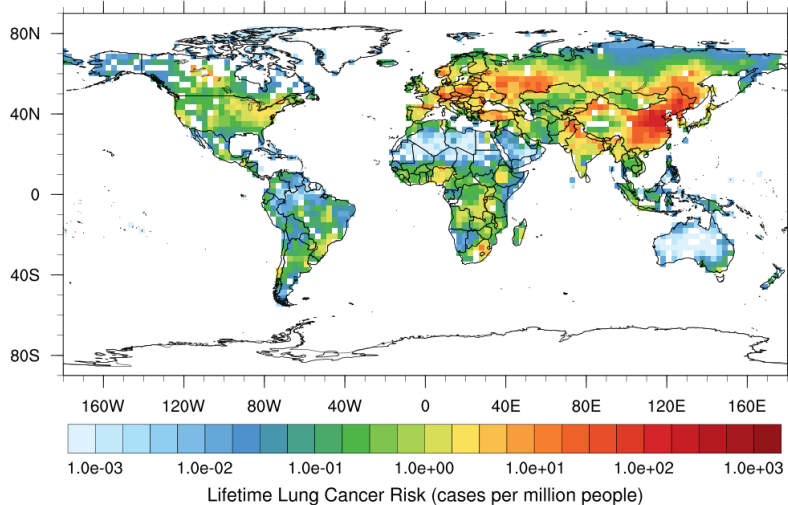


### A. Vertical profile of global mean BaP concentration



### B. Estimated lifetime lung cancer risks

#### (i) Additional cancer cases per million people exposed





**(ii) Additional cancer cases per km<sup>2</sup> exposed area**

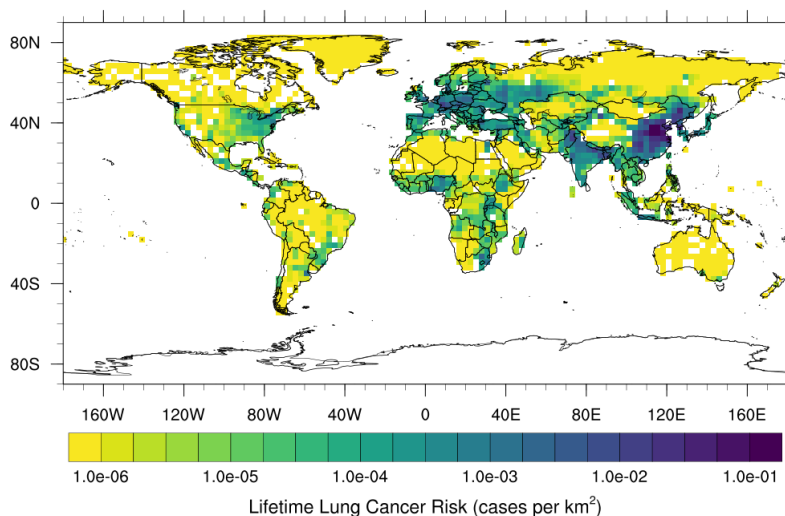


**Figure 2.** A: Vertical profiles of global mean BaP volume mixing ratio (pptv) averaged over the period 2007-2009 and obtained with different kinetic schemes (Mu et al. 2018 (ROI-T), Pöschl et al. 2001, Kwamena et al. 2004, Kahan et al. 2006). B: Estimated lifetime lung cancer risks (LLCR) for BaP as additional cancer cases (i) per million people exposed over a lifetime of 70 years, and (ii) per km<sup>2</sup> of exposed area based on BaP concentrations obtained with the ROI-T scheme.

***Lifetime lung cancer risk***

Figure 2B shows the lifetime lung cancer risk (LLCR) estimates due to the exposure to BaP alone. LLCR is derived from the ROI-T predicted near-surface BaP concentrations and a unit-risk (UR) for lung cancer upon chronic exposure to 1 ng m<sup>-3</sup> BaP over a lifetime of 70 years. The US EPA<sup>60</sup>, cited by WHO<sup>61</sup>, estimated a UR of  $8.7 \times 10^{-5}$  per ng m<sup>-3</sup>, which is comparable to the estimate produced by the National Institute for Public Health and the Environment of the Netherlands<sup>62</sup> (UR =  $10 \times 10^{-5}$  per ng m<sup>-3</sup>). The WHO unit risk is used to estimate the LLCR value according to the following equation.

$$LLCR = UR \times [\text{BaP}]$$



where [BaP] is the 3-year average (2007-2009) near-surface concentration of BaP ( $\text{ng m}^{-3}$ ). Note that this calculation of lifetime cancer risk assumes steady near-surface concentrations over the entire lifetime and does not consider the cancer risk by exposure to chemical transformation products of BaP, as discussed further below. Moreover, the LLCR due to BaP alone, as presented in this study, only represents a fraction and at most a lower estimate of the LLCR due to total air pollution. BaP is co-emitted with other carcinogenic polycyclic aromatic compounds of various atmospheric lifetime and carcinogenicity of photochemical products, and does not dominate carcinogenicity of polluted air<sup>63, 64</sup>.

The estimated LLCR from BaP exposure is very low ( $<1 \times 10^{-8}$ ) in parts of North Africa and Australia, while we find the highest risk in Central, Eastern, and Northeastern China, exceeding  $1 \times 10^{-4}$ , or 100 excess cases per million people. Elevated risk (1-100 excess cases) is seen in northeast America, central, eastern and southeastern Europe, parts of Eastern and South Africa and Nigeria, parts of Brazil, Argentina and Chile, western southern parts of the Russian Far East, China, and the Indus and Gangetic Plains (Southern Asia). Due to its influence on BaP distribution in air, the choice of degradation scheme has a pronounced influence on the estimated lung cancer risk (SI S6). When combined with population density<sup>65</sup> (Figure 2B(ii)), higher risks ( $>1 \times 10^{-2}$  additional cases per  $\text{km}^2$ ) are observed in densely populated regions, notably in China, India, Pakistan, central and eastern Europe, Nigeria, South Africa and eastern US (between  $1 \times 10^{-4}$ - $1 \times 10^{-2}$  cases per  $\text{km}^2$ ). In remote regions, the lung cancer risks are usually below  $1 \times 10^{-6}$  additional cases per  $\text{km}^2$ . Considering population density and its correlation with LLCR is crucial for formulating effective public health policies and interventions to mitigate BaP-related health implications.

A limitation related to the model's spatial resolution is related to the spatial variability of BaP concentrations at scales smaller than the model grid size, also known as subgrid variability (SGV). As BaP is a primary pollutant, its near-surface SGV is caused by the spatial heterogeneity of the emission sources, which can be large in polluted areas<sup>66</sup>. In such areas, where both population density and emission sources are concentrated, i.e., urban environments, SGV can lead to a systematic underestimation of LLCR. Conversely, in regions where population centers and emission sources are evenly distributed across a grid cell, the error



introduced by SGV will be small. A possible approach to address this constraint involves spatial downscaling, using high-resolution population data to disaggregate emissions onto a finer resolution grid.

#### 4. Implications & Outlook

The atmospheric degradation, persistence, long-range atmospheric transport potential, and compartmental distribution of BaP are very sensitive to temperature and relative humidity. This study improves our understanding and prediction of the atmospheric fate and large-scale distribution of BaP and other organic pollutants which are carried by aerosols and subject to heterogeneous reactivity. The efficiency of shielding from photochemistry, which can vary significantly between regions, shapes the pollutant's distribution and long-range transport potential. These factors, already more sensitive than previously anticipated,<sup>67</sup> are expected to change under a changing climate. The effect of future climate on BaP reactivity and, hence, lifetime in various parts of the atmosphere, remains to be investigated. Oxygenated BaPs, which are formed during the oxidation reaction of BaP with O<sub>3</sub>, are known to have toxicological and physicochemical properties that can contribute to, or even enhance, the overall adverse effects of BaP on human and ecosystem health. To achieve a more comprehensive health risk assessment, future research could explore and incorporate the toxicity of these products. The dependence of BaP reactivity on temperature and relative humidity demonstrated in this study suggests that individuals living in warm and humid climates may be exposed to air with a comparatively higher fraction of BaP oxidation products (that have been formed from photochemical reaction of BaP). Further quantitative estimates of the global distribution of BaP oxidation products will require data on photochemical yields and degradation kinetics, which are currently lacking. The distribution of oxidation products of BaP in near-surface (i.e., inhaled) air should be used to study the related cancer risks for exposed populations. This will also require an estimate of the unit risk of BaP oxidation products. Apart from BaP, other PM constituents contribute to the carcinogenicity of ambient air.<sup>68, 69</sup> Little is known about these substances' reactivity. As a number of suspects are polycyclic aromatic compounds,<sup>70, 71</sup> the here presented implications on atmospheric fate may apply for a range of hazardous pollutants.

#### Supporting Information

Descriptions of different parameterization schemes of BaP multiphase degradation rates (Tables S1-S2), spatial distribution of BaP atmospheric column burden (Figure S1), model



performance evaluation (Figures S2-S3), vertical profiles of regional-mean BaP (Figure S4), global and regional mean of BaP atmospheric burdens and their respective lifetimes (Tables S3-S4), global and regional mean of BaP burden across soil, vegetation, and ocean compartments (Table S5), spatial distributions of lifetime lung cancer risks (Figure S5).

### Acknowledgments

This work was funded by the Max Planck Society (MPG). We acknowledge high-performance computing support from the Max Planck Computing and Data Facility. MO has received funding for part of this work through the Helmholtz Association's Initiative and Networking Fund (no. VH-NG-1533).

### References

1. Boström, C.-E.; Gerde, P.; Hanberg, A.; Jernström, B.; Johansson, C.; Kyrklund, T.; Rannug, A.; Törnqvist, M.; Victorin, K.; Westerholm, R., Cancer risk assessment, indicators, and guidelines for polycyclic aromatic hydrocarbons in the ambient air. *Environ. Health Perspect.* **2002**, *110* (Suppl 3), 451-488.
2. Keyte, I. J.; Harrison, R. M.; Lammel, G., Chemical reactivity and long-range transport potential of polycyclic aromatic hydrocarbons - a review. *Chem. Soc. Rev.* **2013**, *42* (24), 9333-9391.
3. Pöschl, U.; Shiraiwa, M., Multiphase Chemistry at the Atmosphere–Biosphere Interface Influencing Climate and Public Health in the Anthropocene. *Chem. Rev.* **2015**, *115* (10), 4440-4475.
4. IARC, A review of human carcinogens. In *Part F: Chemical agents and related occupations* [Online] World Health Organization: Lyon, France, 2012; p. 628. <https://monographs.iarc.who.int/wp-content/uploads/2018/06/mono100F.pdf> (accessed 03/11/2022).
5. Khaiwal, R.; Sokhi, R.; Van Grieken, R., Atmospheric polycyclic aromatic hydrocarbons: Source attribution, emission factors and regulation. *Atmos. Environ.* **2008**, *42* (13), 2895-2921.
6. European Union, Directive 2004/107/EC of the European Parliament and of the Council of 15 December 2004 relating to arsenic, cadmium, mercury, nickel and polycyclic aromatic hydrocarbons in ambient air. Office Journal of the European Union: 2005; p 14.
7. Lammel, G.; Sehili, A. M.; Bond, T. C.; Feichter, J.; Grassl, H., Gas/particle partitioning and global distribution of polycyclic aromatic hydrocarbons – A modelling approach. *Chemosphere* **2009**, *76* (1), 98-106.



8. Friedman, C. L.; Selin, N. E., Long-range atmospheric transport of polycyclic aromatic hydrocarbons: a global 3-D model analysis including evaluation of Arctic sources. *Environ. Sci. Technol.* **2012**, *46* (17), 9501-9510.
9. Friedman, C. L.; Pierce, J. R.; Selin, N. E., Assessing the influence of secondary organic versus primary carbonaceous aerosols on long-range atmospheric polycyclic aromatic hydrocarbon transport. *Environ. Sci. Technol.* **2014**, *48* (6), 3293-3302.
10. Galarneau, E.; Makar, P. A.; Zheng, Q.; Narayan, J.; Zhang, J.; Moran, M. D.; Bari, M. A.; Pathela, S.; Chen, A.; Chlumsky, R., PAH concentrations simulated with the AURAMS-PAH chemical transport model over Canada and the USA. *Atmos. Chem. Phys.* **2014**, *14* (8), 4065-4077.
11. Efsthathiou, C. I.; Matejovičová, J.; Bieser, J.; Lammel, G., Evaluation of gas-particle partitioning in a regional air quality model for organic pollutants. *Atmos. Chem. Phys.* **2016**, *16* (23), 15327-15345.
12. Mu, Q.; Shiraiwa, M.; Octaviani, M.; Ma, N.; Ding, A.; Su, H.; Lammel, G.; Pöschl, U.; Cheng, Y., Temperature effect on phase state and reactivity controls atmospheric multiphase chemistry and transport of PAHs. *Sci. Adv.* **2018**, *4* (3).
13. Thackray, C. P.; Friedman, C. L.; Zhang, Y.; Selin, N. E., Quantitative assessment of parametric uncertainty in Northern Hemisphere PAH concentrations. *Environ. Sci. Technol.* **2015**, *49* (15), 9185-9193.
14. Shiraiwa, M.; Garland, R. M.; Pöschl, U., Kinetic double-layer model of aerosol surface chemistry and gas-particle interactions (K2-SURF): Degradation of polycyclic aromatic hydrocarbons exposed to O<sub>3</sub>, NO<sub>2</sub>, H<sub>2</sub>O, OH and NO<sub>3</sub>. *Atmos. Chem. Phys.* **2009**, *9* (24), 9571-9586.
15. Zhou, S.; Shiraiwa, M.; McWhinney, R. D.; Pöschl, U.; Abbatt, J. P. D., Kinetic limitations in gas-particle reactions arising from slow diffusion in secondary organic aerosol. *Faraday Discuss.* **2013**, *165* (0), 391-406.
16. Shrivastava, M.; Lou, S.; Zelenyuk, A.; Easter, R. C.; Corley, R. A.; Thrall, B. D.; Rasch, P. J.; Fast, J. D.; Massey Simonich, S. L.; Shen, H.; Tao, S., Global long-range transport and lung cancer risk from polycyclic aromatic hydrocarbons shielded by coatings of organic aerosol. *Proc. Natl. Acad. Sci.* **2017**, *114* (6), 1246-1251.
17. Armstrong, B.; Hutchinson, E.; Unwin, J.; Fletcher, T., Lung Cancer Risk after Exposure to Polycyclic Aromatic Hydrocarbons: A Review and Meta-Analysis. *Environ. Health Perspect.* **2004**, *112* (9), 970-978.
18. Kelly, J. M.; Ivatt, P. D.; Evans, M. J.; Kroll, J. H.; Hrdina, A. I. H.; Kohale, I. N.; White, F. M.; Engelward, B. P.; Selin, N. E., Global Cancer Risk From Unregulated Polycyclic Aromatic Hydrocarbons. *GeoHealth* **2021**, *5* (9), e2021GH000401.
19. Lou, S.; Shrivastava, M.; Ding, A.; Easter, R. C.; Fast, J. D.; Rasch, P. J.; Shen, H.; Massey Simonich, S. L.; Smith, S. J.; Tao, S.; Zelenyuk, A., Shift in Peaks of PAH-Associated





Health Risks From East Asia to South Asia and Africa in the Future. *Earth's Future* **2023**, *11* (6), e2022EF003185.

20. Pöschl, U., Formation and Decomposition of Hazardous Chemical Components Contained in Atmospheric Aerosol Particles. *Journal of Aerosol Medicine* **2002**, *15* (2), 203-212.

21. Yu, D.; Penning, T. M.; Field, J. M.; Berlin, J. A., Benzo[ a ]pyrene-7,8-dione is More Mutagenic than Anti -BPDE on p53 and is Dependent on the Generation of Reactive Oxygen Species. *Polycycl. Aromat. Comp.* **2002**, *22* (3-4), 881-891.

22. Pitts, J. N.; Lokensgard, D. M.; Ripley, P. S.; Van Cauwenberghe, K. A.; Van Vaeck, L.; Shaffer, S. D.; Thill, A. J.; Belser, W. L., ``Atmospheric" Epoxidation of Benzo[a]pyrene by Ozone: Formation of the Metabolite Benzo[a]pyrene-4,5-oxide. *Science* **1980**, *210* (4476), 1347-1349.

23. Koeber, R.; Bayona, J. M.; Niessner, R., Determination of Benzo[a]pyrene Diones in Air Particulate Matter with Liquid Chromatography Mass Spectrometry. *Environ. Sci. Technol.* **1999**, *33* (10), 1552-1558.

24. Li, Y.; Juhasz, A. L.; Ma, L. Q.; Cui, X., Inhalation bioaccessibility of PAHs in PM2.5: Implications for risk assessment and toxicity prediction. *Sci. Total Environ.* **2019**, *650*, 56-64.

25. Burdick, A. D.; Davis, J. W., II; Liu, K. J.; Hudson, L. G.; Shi, H.; Monske, M. L.; Burchiel, S. W., Benzo(a)pyrene Quinones Increase Cell Proliferation, Generate Reactive Oxygen Species, and Transactivate the Epidermal Growth Factor Receptor in Breast Epithelial Cells. *Cancer Research* **2003**, *63* (22), 7825-7833.

26. Fertuck, K. C.; Matthews, J. B.; Zacharewski, T. R., Hydroxylated Benzo[a]pyrene Metabolites Are Responsible for in Vitro Estrogen Receptor-Mediated Gene Expression Induced by Benzo[a]pyrene, but Do Not Elicit Uterotrophic Effects in Vivo. *Toxicological Sciences* **2001**, *59* (2), 231-240.

27. Jöckel, P.; Kerkweg, A.; Pozzer, A.; Sander, R.; Tost, H.; Riede, H.; Baumgaertner, A.; Gromov, S.; Kern, B., Development cycle 2 of the Modular Earth Submodel System (MESSy2). *Geosci. Model Dev.* **2010**, *3* (2), 717-752.

28. Jöckel, P.; Tost, H.; Pozzer, A.; Brühl, C.; Buchholz, J.; Ganzeveld, L.; Hoor, P.; Kerkweg, A.; Lawrence, M. G.; Sander, R.; Steil, B.; Stiller, G.; Tanarhte, M.; Taraborrelli, D.; van Aardenne, J.; Lelieveld, J., The atmospheric chemistry general circulation model ECHAM5/MESSy1: consistent simulation of ozone from the surface to the mesosphere. *Atmos. Chem. Phys.* **2006**, *6* (12), 5067-5104.

29. Octaviani, M.; Tost, H.; Lammel, G., Global simulation of semivolatile organic compounds – development and evaluation of the MESSy submodel SVOC (v1.0). *Geosci. Model Dev.* **2019**, *12* (8), 3585-3607.



30. Roeckner, E.; Brokopf, R.; Esch, M.; Giorgetta, M.; Hagemann, S.; Kornblueh, L.; Manzini, E.; Schlese, U.; Schulzweida, U., Sensitivity of simulated climate to horizontal and vertical resolution in the ECHAM5 atmosphere model. *J. Climate* **2006**, *19* (16), 3771-3791.
31. Sander, R.; Baumgaertner, A.; Gromov, S.; Harder, H.; Jöckel, P.; Kerkweg, A.; Kubistin, D.; Regelin, E.; Riede, H.; Sandu, A.; Taraborrelli, D.; Tost, H.; Xie, Z. Q., The atmospheric chemistry box model CAABA/MECCA-3.0. *Geosci. Model Dev.* **2011**, *4* (2), 373-380.
32. Pringle, K. J.; Tost, H.; Message, S.; Steil, B.; Giannadaki, D.; Nenes, A.; Fountoukis, C.; Stier, P.; Vignati, E.; Lelieveld, J., Description and evaluation of GMXe: a new aerosol submodel for global simulations (v1). *Geosci. Model Dev.* **2010**, *3* (2), 391-412.
33. Tsimpidi, A. P.; Karydis, V. A.; Pozzer, A.; Pandis, S. N.; Lelieveld, J., ORACLE 2-D (v2.0): an efficient module to compute the volatility and oxygen content of organic aerosol with a global chemistry-climate model. *Geosci. Model Dev.* **2018**, *11* (8), 3369-3389.
34. Shen, H.; Huang, Y.; Wang, R.; Zhu, D.; Li, W.; Shen, G.; Wang, B.; Zhang, Y.; Chen, Y.; Lu, Y.; Chen, H.; Li, T.; Sun, K.; Li, B.; Liu, W.; Liu, J.; Tao, S., Global atmospheric emissions of polycyclic aromatic hydrocarbons from 1960 to 2008 and future predictions. *Environ. Sci. Technol.* **2013**, *47* (12), 6415-6424.
35. van Vuuren, D. P.; Edmonds, J.; Kainuma, M.; Riahi, K.; Thomson, A.; Hibbard, K.; Hurtt, G. C.; Kram, T.; Krey, V.; Lamarque, J.-F.; Masui, T.; Meinshausen, M.; Nakicenovic, N.; Smith, S. J.; Rose, S. K., The representative concentration pathways: an overview. *Clim. Change* **2011**, *109* (1), 5.
36. Goss, K.-U.; Schwarzenbach, R. P., Linear free energy relationships used to evaluate equilibrium partitioning of organic compounds. *Environ. Sci. Technol.* **2001**, *35* (1), 1-9.
37. Shahpoury, P.; Lammel, G.; Albinet, A.; Sofuoğlu, A.; Dumanoglu, Y.; Sofuoğlu, S. C.; Wagner, Z.; Zdimas, V., Evaluation of a conceptual model for gas-particle partitioning of polycyclic aromatic hydrocarbons using polyparameter linear free energy relationships. *Environ. Sci. Technol.* **2016**, *50* (22), 12312-12319.
38. Shiraiwa, M.; Sosedova, Y.; Rouvière, A.; Yang, H.; Zhang, Y.; Abbatt, J. P. D.; Ammann, M.; Pöschl, U., The role of long-lived reactive oxygen intermediates in the reaction of ozone with aerosol particles. *Nat. Chem.* **2011**, *3* (4), 291-295.
39. Berkemeier, T.; Steimer, S. S.; Krieger, U. K.; Peter, T.; Pöschl, U.; Ammann, M.; Shiraiwa, M., Ozone uptake on glassy, semi-solid and liquid organic matter and the role of reactive oxygen intermediates in atmospheric aerosol chemistry. *Phys. Chem. Chem. Phys.* **2016**, *18* (18), 12662-12674.
40. Koop, T.; Bookhold, J.; Shiraiwa, M.; Pöschl, U., Glass transition and phase state of organic compounds: dependency on molecular properties and implications for secondary organic aerosols in the atmosphere. *Phys. Chem. Chem. Phys.* **2011**, *13* (43), 19238-19255.



41. Pöschl, U.; Rudich, Y.; Ammann, M., Kinetic model framework for aerosol and cloud surface chemistry and gas-particle interactions - Part 1: General equations, parameters, and terminology. *Atmos. Chem. Phys.* **2007**, *7* (23), 5989-6023.
42. Shiraiwa, M.; Ammann, M.; Koop, T.; Pöschl, U., Gas uptake and chemical aging of semisolid organic aerosol particles. *Proc. Natl. Acad. Sci.* **2011**, *108* (27), 11003-11008.
43. Shiraiwa, M.; Li, Y.; Tsimpidi, A. P.; Karydis, V. A.; Berkemeier, T.; Pandis, S. N.; Lelieveld, J.; Koop, T.; Pöschl, U., Global distribution of particle phase state in atmospheric secondary organic aerosols. *Nat. Commun.* **2017**, *8*, 15002.
44. Shiraiwa, M.; Pfrang, C.; Pöschl, U., Kinetic multi-layer model of aerosol surface and bulk chemistry (KM-SUB): the influence of interfacial transport and bulk diffusion on the oxidation of oleic acid by ozone. *Atmos. Chem. Phys.* **2010**, *10* (8), 3673-3691.
45. Pöschl, U.; Letzel, T.; Schauer, C.; Niessner, R., Interaction of ozone and water vapor with spark discharge soot aerosol particles coated with benzo[a]pyrene: O<sub>3</sub> and H<sub>2</sub>O adsorption, benzo[a]pyrene degradation, and atmospheric Implications. *J. Phys. Chem. A* **2001**, *105* (16), 4029-4041.
46. Kwamena, N.-O. A.; Thornton, J. A.; Abbatt, J. P. D., Kinetics of surface-bound benzo[a]pyrene and ozone on solid organic and salt aerosols. *J. Phys. Chem. A* **2004**, *108* (52), 11626-11634.
47. Kahan, T. F.; Kwamena, N. O. A.; Donaldson, D. J., Heterogeneous ozonation kinetics of polycyclic aromatic hydrocarbons on organic films. *Atmos. Environ.* **2006**, *40* (19), 3448-3459.
48. BioHCWin v1.01 *Biodegradation Prediction of Petroleum Hydrocarbons v1.01*, U.S. Environmental Protection Agency, Office of Pollution Prevention and Toxics: Washington DC, 2008.
49. Park, K. S.; Sims, R. C.; Dupont, R. R.; Doucette, W. J.; Matthews, J. E., Fate of PAH compounds in two soil types: Influence of volatilization, abiotic loss and biological activity. *Environ. Toxicol. Chem.* **1990**, *9* (2), 187-195.
50. Ikeda, K.; Tanimoto, H.; Sugita, T.; Akiyoshi, H.; Kanaya, Y.; Zhu, C.; Taketani, F., Tagged tracer simulations of black carbon in the Arctic: transport, source contributions, and budget. *Atmos. Chem. Phys.* **2017**, *17* (17), 10515-10533.
51. Stohl, A., Characteristics of atmospheric transport into the Arctic troposphere. *J. Geophys. Res. (Atmos.)* **2006**, *111* (D11), D11306.
52. Becker, S.; Halsall, C. J.; Tych, W.; Hung, H.; Attewell, S.; Blanchard, P.; Li, H.; Fellin, P.; Stern, G.; Billeck, B.; Friesen, S., Resolving the long-term trends of polycyclic aromatic hydrocarbons in the Canadian Arctic atmosphere. *Environ. Sci. Technol.* **2006**, *40* (10), 3217-3222.



53. Laender, F. D.; Hammer, J.; Hendriks, A. J.; Soetaert, K.; Janssen, C. R., Combining monitoring data and modeling identifies PAHs as emerging contaminants in the Arctic. *Environ. Sci. Technol.* **2011**, *45* (20), 9024-9029.
54. Kukučka, P.; Lammel, G.; Dvorská, A.; Klánová, J.; Möller, A.; Fries, E., Contamination of Antarctic snow by polycyclic aromatic hydrocarbons dominated by combustion sources in the polar region. *Environ. Chem.* **2010**, *7* (6), 504-513.
55. Barbaro, E.; Zangrando, R.; Kirchgeorg, T.; Bazzano, A.; Illuminati, S.; Annibaldi, A.; Rella, S.; Truzzi, C.; Grotti, M.; Ceccarini, A.; Malitesta, C.; Scarponi, G.; Gambaro, A., An integrated study of the chemical composition of Antarctic aerosol to investigate natural and anthropogenic sources. *Environ. Chem.* **2016**, *13* (5), 867-876.
56. Matthias, V.; Aulinger, A.; Quante, M., CMAQ simulations of the benzo(a)pyrene distribution over Europe for 2000 and 2001. *Atmos. Environ.* **2009**, *43* (26), 4078-4086.
57. Aulinger, A.; Matthias, V.; Quante, M., An approach to temporally disaggregate benzo(a)pyrene emissions and their application to a 3D Eulerian atmospheric chemistry transport model. *Water Air Soil Pollut.* **2011**, *216* (1), 643-655.
58. Bieser, J.; Aulinger, A.; Matthias, V.; Quante, M., Impact of emission reductions between 1980 and 2020 on atmospheric benzo[a]pyrene concentrations over Europe. *Water Air Soil Pollut.* **2012**, *223* (3), 1393-1414.
59. San José, R.; Pérez, J. L.; Callén, M. S.; López, J. M.; Mastral, A., BaP (PAH) air quality modelling exercise over Zaragoza (Spain) using an adapted version of WRF-CMAQ model. *Environ. Pollut.* **2013**, *183*, 151-158.
60. U.S. EPA. *Health Effects Assessment for Benzo[a]pyrene*; U.S. Environmental Protection Agency: Washington, DC, 1986; p 42.
61. WHO *Air quality guidelines for Europe, 2nd Ed.*; World Health Organization. Regional Office for Europe: Copenhagen, 2000; p 288.
62. RIVM *Integrated Criteria Document PAHs*; National Institute of Public Health and Environmental Protection.: Bilthoven, The Netherlands, 1989; p 408.
63. Liu, B.; Xue, Z.; Zhu, X.; Jia, C., Long-term trends (1990–2014), health risks, and sources of atmospheric polycyclic aromatic hydrocarbons (PAHs) in the U.S. *Environ. Pollut.* **2017**, *220*, 1171-1179.
64. Zhang, X.; Wang, X.; Zhao, X.; Tang, Z.; Liang, W.; Wu, X.; Wang, J.; Wang, X.; Niu, L., Important But Overlooked Potential Risks of Substituted Polycyclic Aromatic Hydrocarbon: Looking Below the Tip of the Iceberg. *Reviews Env. Contamination (formerly:Residue Reviews)* **2022**, *260* (1), 18.
65. Doxsey-Whitfield, E.; MacManus, K.; Adamo, S. B.; Pistolesi, L.; Squires, J.; Borkovska, O.; Baptista, S. R., Taking Advantage of the Improved Availability of Census Data:



A First Look at the Gridded Population of the World, Version 4. *Papers in Applied Geography* **2015**, *1* (3), 226-234.

66. Qian, Y.; Gustafson Jr, W. I.; Fast, J. D., An investigation of the sub-grid variability of trace gases and aerosols for global climate modeling. *Atmos. Chem. Phys.* **2010**, *10* (14), 6917-6946.

67. Friedman, C. L.; Zhang, Y.; Selin, N. E., Climate change and emissions impacts on atmospheric PAH transport to the Arctic. *Environ. Sci. Technol.* **2013**, *48* (1), 429-437.

68. IARC, Some non-heterocyclic polycyclic aromatic hydrocarbons and some related exposures. IARC monographs on the evaluation of carcinogenic risks to humans ed.; World Health Organization: Lyon, France, 2010; p. 853. [https://publications.iarc.fr/\\_publications/media/download/2841/a076b09df49aeeb8c7922378fe4f372fda3edd13.pdf](https://publications.iarc.fr/_publications/media/download/2841/a076b09df49aeeb8c7922378fe4f372fda3edd13.pdf) (accessed 05/2024).

69. IARC, Diesel and gasoline engine exhausts and some nitroarenes. IARC monographs on the evaluation of carcinogenic risks to humans ed.; World Health Organization: Lyon, France, 2012; p. 714. [https://publications.iarc.fr/\\_publications/media/download/3181/e6bd0692f1a9bb46589d3ca2d8178fa8dcd05ba5.pdf](https://publications.iarc.fr/_publications/media/download/3181/e6bd0692f1a9bb46589d3ca2d8178fa8dcd05ba5.pdf) (accessed 05/2024).

70. Richter-Brockmann, S.; Achten, C., Analysis and toxicity of 59 PAH in petrogenic and pyrogenic environmental samples including dibenzopyrenes, 7H-benzo[c]fluorene, 5-methylchrysene and 1-methylpyrene. *Chemosphere* **2018**, *200*, 495-503.

71. Li, T.; Su, W.; Zhong, L.; Liang, W.; Feng, X.; Zhu, B.; Ruan, T.; Jiang, G., An Integrated Workflow Assisted by In Silico Predictions To Expand the List of Priority Polycyclic Aromatic Compounds. *Environ. Sci. Technol.* **2023**, *57* (49), 20854-20863.